Available online at www.sciencedirect.com
ScienceDirect
Journal of Sound and Vibration 308 (2007) 268–286
JOURNAL OF SOUND AND VIBRATION
www.elsevier.com/locate/jsvi

Free vibration of laminated and sandwich plates using enhanced plate theories

J.-S. Kim*

Department of Aerospace Engineering, The Pennsylvania State University, University Park, PA 16802, USA

Received 6 January 2006; received in revised form 7 October 2006; accepted 24 July 2007
Available online 4 September 2007

Abstract

In this paper two enhanced plate theories for laminated and sandwich plates are developed via the mixed variational formulation for free vibration studies. A concept presented by the author [J.-S. Kim, Reconstruction of first-order shear deformation theory for laminated and sandwich shells, *AIAA Journal* 42 (2004) 1685–1697], which includes the displacement and stress recovery procedure, is extended to the mixed variational theorem. By obtaining the transverse shear stresses based on higher-order zig-zag theories, the mixed variational formulation embraces them as the classical FSDT and HSDT. Relationships between the higher-order zig-zag theories and the classical FSDT and HSDT are systematically established via the mixed variational theorem and the generalized definition of the mean displacement. The accuracy and efficiency of the present enhanced plate theories are demonstrated by comparing their results with the reported results in the literature and 3D exact elasticity solutions for the plates vibrating in cylindrical bending.

1. Introduction

Laminated composite materials provide excellent opportunities for light weight and high stiffness structures as well as elastic couplings for potential optimization of design criteria. Many models accounting for the transverse shear deformation in composite and sandwich plates have appeared in the literature, since the transverse shear stiffness of these materials is very low as compared to their in-plane rigidity. It is a challenging problem to understand the dynamical behavior of laminated and sandwich plates with sufficient accuracy, especially for composite sandwich structures due to the strong shearing of a foam core.

Since the first-order shear deformation theory (FSDT) was proposed by Reissner [1,2] and Mindlin [3], several studies using FSDT have been conducted for the free vibration analysis of composite plates [4–7]. In the vibration analysis of isotropic moderately thick plates, the FSDT will usually suffice. It is, however, inadequate to model the dynamical behavior of highly orthotropic, composite or sandwich plates using the FSDT, unless appropriate shear correction factors (SCFs) are provided [8]. Thus many plate theories have been developed to overcome the deficiency of FSDT.

*Tel.: +1 814 865 1986; fax: +1 814 865 1991.
E-mail address: jskim@psu.edu

0022-460X/$ - see front matter © 2007 Elsevier Ltd. All rights reserved.
doi:10.1016/j.jsv.2007.07.040

Smeared displacement-based higher-order shear deformation theories were developed first [9–15]. The assumed displacement of these higher-order theories is expressed as a polynomial form of the thickness coordinate. These theories do not account for continuity of the transverse shear stresses and cannot accurately describe the through-the-thickness variation of stresses. A better description can be obtained by layerwise theories [16–18] that are known to be fairly accurate since they allow a kink in the slope of deflection at each interface between layers. These layerwise theories, however, have the drawback of requiring many degrees of freedom depending upon the number of layers. Higher-order zig-zag theories, which are constructed by superimposing a linear zig-zag displacement proposed by Yu [19] and DiSciuva [20] on overall cubic varying fields, have been paid attentions because of their accuracy and efficiency in the ply-level analysis [21–24]. They satisfy not only the traction free conditions at the top and bottom surface but also the continuity conditions at the interface. Assessments of zig-zag theories for composite plates and shells can be found in the recent review paper by Carrera [25], where the original contributions of Lekhnitskii and Ambartsumian to zig-zag theories are discussed in detail.

There have been several efforts to keep the same computational cost as the FSDT in predicting the structural behavior of laminated composites. One of them is to find the appropriate SCFs for laminated composites [26,27]. As is well known, the global response by the FSDT with an appropriate SCFs is fairly good, even for thick laminated composites. Burton and Noor [28] proposed a predictor–corrector method for laminated and sandwich shells. The displacement fields have been calculated by integrating the equilibrium equation, in which the SCFs are obtained by an iterative manner in predictor phase, through the thickness in corrector phase. A post-process method has been developed by Cho and Kim [29]. An efficient higher-order plate theory (EHOPT) developed by Cho and Parmerter [21,22] is utilized as a post-processor. They found the relationship between the FSDT with SCFs and the EHOPT under the assumption of the transverse shear energy equivalence. This method has been extended to general lamination configurations [30], various post-processors [31] and the finite element method [32,33]. Accuracy of both predictor–corrector and post-process methods strongly depends on the SCFs.

On the other hand, several FSDT type plate theories have been developed by improving the transverse shear strains. Qi and Knight [34,35] have developed a refined FSDT for laminated plates. They introduced the effective shear stress and strain so that the actual shear stress and strain are expressed in terms of the averaged shear strain of the original FSDT. An accurate asymptotically correct shear deformation theory, which is based on the variational-asymptotic method originally proposed by Berdichevsky [36], was proposed by Sutyrin [37]. As he pointed out, however, the variational-asymptotic technique leads to a theory with higher derivatives, which is asymptotically correct but not useful because of its being overly complex. Yu et al. [38] have, recently, developed a nonlinear ''Reissner-Like'' plate theory based on the variational-asymptotic method. They have developed the computer program based on this, called variational asymptotic plate and shell theory (VAPAS) [39], by incorporating the one-dimensional (1-D) through-the-thickness finite element analysis to overcome the analytical complexity of variational-asymptotic procedure. Recently, Yu [40] extended this theory to allow maximum freedom for the asymptotically correct energy transformation. An enhanced first-order shear deformation theory (EFSDT) has been developed by the author and his co-worker [41], which is based on the definition of Reissner–Mindlin's plate theory. It was assumed that the displacement and in-plain strain fields of the FSDT can approximate those of three-dimensional (3D) theory in the averaged least square sense. This theory has also been improved by minimizing the truncated strain energy [42,43].

In this paper, a concept presented by the author [42], which includes the displacement and stress recovery procedure, is extended to the mixed variational theorem [2,44]. There are a couple of papers dealing with such a mixed variational approach. Murakami [45] used such a approach by introducing a function of the thickness coordinate to emulate the zig-zag effect [46,47]. This was extended to the dynamic analysis of plates and shells by Carrera that included the effect of transverse normal stress [48]. Generalized mixed-based plate theories have been developed by Messina [49] and Messina and Soldatos [50], where the importance of completely fulfilling the transverse shear stress continuity was well discussed. Tarn and Wang [51] developed a refined asymptotic theory in the frame work of the Hellinger–Reissner variational functional, in which the displacements and transverse stresses were taken to be the functions subject to variation. The present work is mainly inspired by Tarn and Wang's work [51] and the author's previous work [41–43].

In this context, the present work includes the following aspects:

(1) The mixed variational formulation [51] is adopted with the assumption of a negligible transverse normal stress.
(2) Transverse shear stresses used in the mixed formulation are derived from higher-order zig-zag theories based on Refs. [21,22].
(3) Displacement fields of the classical FSDT [1,3] and higher-order shear deformation theory (HSDT) [13,15] are used to derive the EFSDT and enhanced HSDT (EHSDT) that preserve the computational advantage of the classical FSDT and HSDT, respectively.
(4) Displacement fields of higher-order zig-zag theories are recovered via the generalized definition of the mean displacement that was established in Ref. [42].
(5) The effectiveness of the present models is demonstrated by comparing their results, such as frequencies and through-the-thickness mode shapes, with the 3D exact elasticity solutions and the data available in literature.

2. Mixed formulation

A laminated plate of thickness h made of a monoclinic material is considered. Geometry and coordinates of a laminated plate is shown in Fig. 1. Unless it is not differently specified, Greek indices will take values in the set 1, 2, whereas Latin indices will take values in 1, 2, 3. The reference two-dimensional (2D) plane is represented by x_α and the through-the-thickness position is denoted by x_3, where $x_3 \in [-h/2, +h/2]$.

The 3D constitutive equation is given by

$$\sigma_{ij} = C_{ijkl}\tfrac{1}{2}(u_{k,l} + u_{l,k}), \tag{1}$$

where σ_{ij} and u_i represent the stress tensor and displacements, respectively. C_{ijkl} denote the components of elasticity tensor with monoclinic symmetry properties. Subscripts $(\,)_{,i}$ denote partial derivatives with respect to x_i coordinates.

The Hellinger–Reissner functional [51] for the problem is expressed as

$$\Pi_R = \int_{-h/2}^{+h/2} \int_\Omega \left[\frac{1}{2}\sigma_{ij}(u_{k,l} + u_{l,k}) - W_c(\sigma_{ij})\right] \mathrm{d}\Omega\, \mathrm{d}x_3 - \int_{S_\sigma} \tilde{T}_i u_i \,\mathrm{d}S_\sigma - \int_{S_u} T_i(u_i - \tilde{u}_i)\,\mathrm{d}S_u, \tag{2}$$

where Ω represents the reference plane, S_σ denotes the boundary with prescribed tractions $\tilde{T}_i$, and S_u denotes the boundary with prescribed displacements $\tilde{u}_i$. $W_c(\sigma_{ij})$ is the complementary energy density function such that $\varepsilon_{ij} = \partial W_c/\partial\sigma_{ij}$, which can be expressed as

$$\varepsilon_{\alpha\beta} = \partial W_c/\partial\sigma_{\alpha\beta} = \tfrac{1}{2}(u_{\alpha,\beta} + u_{\beta,\alpha}), \tag{3}$$

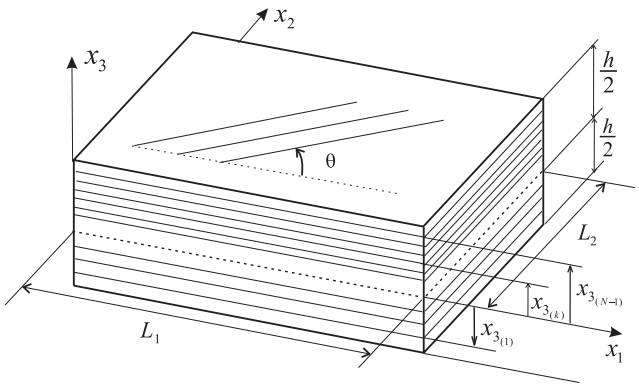

Fig. 1. Geometry and coordinates of laminated plates.

$$\varepsilon_{\alpha 3} = \partial W_c/\partial\sigma_{\alpha 3} = \tfrac{1}{2}C^{-1}_{\alpha 3\beta 3}\sigma_{\beta 3} \equiv \tfrac{1}{2}\gamma^*_{\alpha 3}, \tag{4}$$

$$\varepsilon_{33} = \partial W_c/\partial\sigma_{33} = \frac{1}{C_{3333}}\left\{\sigma_{33} - C_{33\alpha\beta}\frac{1}{2}(u_{\alpha,\beta} + u_{\beta,\alpha})\right\} \equiv \varepsilon^*_{33}, \tag{5}$$

where superscripts $(\,)^*$ are taken to distinguish the transverse strains based on the displacements. The in-plane stresses $\sigma_{\alpha\beta}$ can be expressed by

$$\sigma_{\alpha\beta} = C_{\alpha\beta\gamma\omega}\tfrac{1}{2}(u_{\gamma,\omega} + u_{\omega,\gamma}) + C_{\alpha\beta 33}u_{3,3}. \tag{6}$$

The strains and in-plane stresses are expressed in terms of u_i and σ_{i3} [51], so that the displacements u_i and transverse stresses σ_{i3} are taken to be the functions subject to variations. Substituting Eqs. (3)–(6) into Eq. (2) and taking the first variation yields

$$\begin{aligned}\delta\Pi_R = &\int_{-h/2}^{+h/2}\int_\Omega [\sigma_{\alpha\beta}\delta\varepsilon_{\alpha\beta} + \sigma_{\alpha 3}\delta\gamma_{\alpha 3} + \sigma_{33}\delta\varepsilon_{33} + (\gamma_{\alpha 3} - \gamma^*_{\alpha 3})\delta\sigma_{\alpha 3} + (\varepsilon_{33} - \varepsilon^*_{33})\delta\sigma_{33}]\,\mathrm{d}\Omega\,\mathrm{d}x_3\\ &- \int_{S_\sigma}\tilde{T}_i\delta u_i\,\mathrm{d}S_\sigma - \int_{S_u}\delta T_i(u_i - \tilde{u}_i)\,\mathrm{d}S_u,\end{aligned} \tag{7}$$

in which ε_{ij} represents the strain tensor based on the displacements u_i, while $\gamma^*_{\alpha 3}$ and ε^*_{33} come from the assumed transverse stresses.

Under the assumption of the negligible transverse normal stress, $\sigma_{33} \approx 0$, Eq. (5) yields

$$\varepsilon^*_{33} = -C_{33\alpha\beta}/C_{3333}\tfrac{1}{2}(u_{\alpha,\beta} + u_{\beta,\alpha}) \tag{8}$$

and from the 3D constitutive equation of Eq. (1), $u_{3,3}$ is obtained by

$$u_{3,3} = \varepsilon^*_{33}, \tag{9}$$

which implies that $(\varepsilon_{33} - \varepsilon^*_{33}) = 0$ in Eq. (7).

Plugging Eq. (9) into Eq. (6) yields the 2D in-plane constitutive equations as

$$\sigma_{\alpha\beta} \approx Q_{\alpha\beta\gamma\omega}\tfrac{1}{2}(u_{\gamma,\omega} + u_{\omega,\gamma}) \equiv \sigma^{2D}_{\alpha\beta}, \tag{10}$$

where

$$Q_{\alpha\beta\gamma\omega} = C_{\alpha\beta\gamma\omega} - \frac{C_{\alpha\beta 33}C_{\gamma\omega 33}}{C_{3333}}. \tag{11}$$

With the aid of Eqs. (9) and (10), Eq. (7) can be rewritten as, without the prescribed tractions:

$$\delta\Pi_R|_{\sigma_{33}=0} = \delta\Pi^{2D}_R \equiv \int_\Omega \delta\widehat{\Pi}^{2D}_R\,\mathrm{d}\Omega, \tag{12}$$

in which

$$\delta\widehat{\Pi}^{2D}_R = \langle\sigma^{2D}_{\alpha\beta}\delta\varepsilon_{\alpha\beta} + \sigma_{\alpha 3}\delta\gamma_{\alpha 3} + (\gamma_{\alpha 3} - \gamma^*_{\alpha 3})\delta\sigma_{\alpha 3}\rangle, \tag{13}$$

where $\langle\cdot\rangle = \int_{-h/2}^{+h/2}(\cdot)\,\mathrm{d}x_3$, and the displacement boundary conditions are

$$u_i = \tilde{u}_i \quad \text{on } S_u. \tag{14}$$

The preceding 3D displacement boundary conditions are not easy to exactly satisfy on the boundary, since they involve the boundary layer effect. This is beyond the scope of the present study.

For elastodynamic problems of the plate, the variational principle can be expressed as

$$\int_{t_1}^{t_2}(\delta T - \delta\Pi^{2D}_R)\,\mathrm{d}t = 0, \tag{15}$$

where

$$\delta T = \int_\Omega \delta\widehat{T}\,\mathrm{d}\Omega, \quad \delta\widehat{T} = \langle\rho\dot{u}_i\delta\dot{u}_i\rangle. \tag{16}$$

3. Transverse shear stresses based on higher-order zig-zag theories

In the previous section, two independent fields are assumed for both displacements u_i and transverse shear stresses $\sigma_{\alpha 3}$. In this section, the transverse shear stresses are derived based on higher-order zig-zag theories. The displacement fields, which are well-known FSDT [1,3] and HSDT [13,15], will be discussed in later.

The displacement fields for the perfectly bonded layers can be determined by the requirements, such that the transverse shear stresses should vanish on the upper and lower surface of the plates and should be continuous through the thickness. These conditions can be satisfied by superimposing a linear zig-zag displacement, with a different slope in each layer, on overall cubic or higher varying fields.

One can start with the displacement field that includes a quintic varying displacement and a linear zig-zag displacement:

$$u_\alpha(x_i;t) = \underline{u_\alpha^o(x_\alpha;t) + \psi_\alpha(x_\alpha;t)x_3 + \xi_\alpha(x_\alpha;t)x_3^2 + \phi_\alpha(x_\alpha;t)x_3^3} + \zeta_\alpha(x_\alpha;t)x_3^4 + \eta_\alpha(x_\alpha;t)x_3^5 + \underline{\sum_{k=1}^{N-1} S_\alpha^{(k)}(x_\alpha;t)(x_3 - x_{3(k)})H(x_3 - x_{3(k)})}, \tag{17}$$

$$u_3(x_i;t) = \underline{u_3^o(x_\alpha;t)}, \tag{18}$$

where the superscript, $()^\circ$, represents the variable on the reference plate, N is the number of layers, and $H(x_3 - x_{3(k)})$ is the Heaviside unit step function. The underline terms will be used for EFSDT, whereas the whole expression will be used for EHSDT.

Traction shear-free boundary conditions for the upper and lower surfaces of the plates requires that $\sigma_{\alpha 3}^{\pm} = 0$, where $()^+ = ()|_{x_3=+h/2}, ()^- = ()|_{x_3=-h/2}$. For monoclinic layers, the transverse shear stresses depend only on the transverse shear strains. Thus the traction-free conditions can be written as

$$\gamma_{\alpha 3}^+ = \psi_\alpha + u_{3,\alpha}^o + \xi_\alpha h + \frac{3h^2}{4}\phi_\alpha + \frac{h^3}{2}\zeta_\alpha + \frac{5h^4}{16}\eta_\alpha + \sum_{k=1}^{N-1} S_\alpha^{(k)} = 0, \tag{19}$$

$$\gamma_{\alpha 3}^- = \psi_\alpha + u_{3,\alpha}^o - \xi_\alpha h + \frac{3h^2}{4}\phi_\alpha - \frac{h^3}{2}\zeta_\alpha + \frac{5h^4}{16}\eta_\alpha = 0, \tag{20}$$

which are satisfied by

$$\psi_\alpha + u_{3,\alpha}^o = -\frac{3h^2}{4}\phi_\alpha - \frac{5h^4}{16}\eta_\alpha - \frac{1}{2}\sum_{k=1}^{N-1} S_\alpha^{(k)}, \tag{21}$$

$$\xi_\alpha = -\frac{h^2}{2}\zeta_\alpha - \frac{1}{2h}\sum_{k=1}^{N-1} S_\alpha^{(k)}. \tag{22}$$

The transverse shear strains are then given by

$$\gamma_{\alpha 3} = 3\left(x_3^2 - \frac{h^2}{4}\right)\phi_\alpha + 4x_3\left(x_3^2 - \frac{h^2}{4}\right)\zeta_\alpha + 5\left(x_3^4 - \frac{h^4}{16}\right)\eta_\alpha + \sum_{k=1}^{N-1} S_\alpha^{(k)}\left[-\frac{1}{2} - \frac{x_3}{h} + H(x_3 - x_{3(k)})\right], \tag{23}$$

where $S_\alpha^{(k)}$ represents the change in slope at each interface and depends on the transverse shear material properties. This can be calculated by applying the continuity conditions of transverse shear stresses.

$$\sigma_{\alpha 3}^{(k)}|_{x_3=x_{3(k)}} = \sigma_{\alpha 3}^{(k+1)}|_{x_3=x_{3(k)}} \quad (k = 1, 2, \ldots, N-1). \tag{24}$$

From the preceding equations, one can obtain $2(N-1)$ linear algebraic equations of $2(N-1)$ unknowns $S_\alpha^{(k)}$. By solving this, $S_\alpha^{(k)}$ is obtained by

$$S_\alpha^{(k)} = a_{\alpha\beta}^{(k)}\phi_\beta + b_{\alpha\beta}^{(k)}\zeta_\beta + c_{\alpha\beta}^{(k)}\eta_\beta, \tag{25}$$

where the terms $a_{\alpha\beta}^{(k)}$, $b_{\alpha\beta}^{(k)}$, and $c_{\alpha\beta}^{(k)}$ are functions of the material properties only, and their derivations are given in Appendix A.

The transverse shear strains are then obtained by substituting Eq. (25) into Eq. (23). These can be expressed by

$$\gamma_{\alpha 3} = \underline{\mathscr{A}_{\alpha\beta}\phi_\beta} + \mathscr{B}_{\alpha\beta}\zeta_\beta + \mathscr{C}_{\alpha\beta}\eta_\beta \equiv \gamma_{\alpha 3}^*, \tag{26}$$

in which the underline term, which is the transverse shear strain of a third-order zig-zag plate theory, can be derived by applying the traction free conditions at top and bottom surfaces and continuity conditions to the underline term presented in Eq. (17), and

$$\mathscr{A}_{\alpha\beta} = 3\left(x_3^2 - \frac{h^2}{4}\right)\delta_{\alpha\beta} + \sum_{k=1}^{N-1} a_{\alpha\beta}^{(k)}\left[-\frac{1}{2} - \frac{x_3}{h} + H(x_3 - x_{3(k)})\right], \tag{27}$$

$$\mathscr{B}_{\alpha\beta} = 4x_3\left(x_3^2 - \frac{h^2}{4}\right)\delta_{\alpha\beta} + \sum_{k=1}^{N-1} b_{\alpha\beta}^{(k)}\left[-\frac{1}{2} - \frac{x_3}{h} + H(x_3 - x_{3(k)})\right], \tag{28}$$

$$\mathscr{C}_{\alpha\beta} = 5\left(x_3^4 - \frac{h^4}{16}\right)\delta_{\alpha\beta} + \sum_{k=1}^{N-1} c_{\alpha\beta}^{(k)}\left[-\frac{1}{2} - \frac{x_3}{h} + H(x_3 - x_{3(k)})\right], \tag{29}$$

where $\delta_{\alpha\beta}$ is the Kronecker delta function.

Thus the transverse shear stresses can be written as follows:

$$\sigma_{\alpha 3} = C_{\alpha 3\beta 3}(\underline{\mathscr{A}_{\beta\gamma}\phi_\gamma} + \mathscr{B}_{\beta\gamma}\zeta_\gamma + \mathscr{C}_{\beta\gamma}\eta_\gamma), \tag{30}$$

where all terms are used to obtain the present EHSDT, while the underline term is used for EFSDT.

4. Enhanced plate theories

In this section, two enhanced plate theories, EFSDT and EHSDT, are derived via the mixed variational formulation. The displacement field, which is the classical HSDT, is assumed in the form

$$\bar{u}_\alpha = \underline{\bar{u}_\alpha^o + \theta_\alpha x_3} + \bar{u}_\alpha^h x_3^2 + \theta_\alpha^h x_3^3, \quad \bar{u}_3 = \underline{\bar{u}_3^o}, \tag{31}$$

where the displacements of FSDT and HSDT are denoted by overbar $\bar{u}_i$ to distinguish them from those given in Eqs. (17) and (18), and the underline terms represent the FSDT [1,3]. Notice that the mid-plane displacement $\bar{u}_\alpha^o$ indicates the mean displacement of the plate in the FSDT, while it does not in the HSDT, which will be shown later.

Now we have two required fields, the transverse shear stresses and displacements. Substituting Eqs. (26) and (31) into Eq. (13) yields

$$\delta\widehat{\Pi}_R^{2D} = \underline{N_{\alpha\beta}\delta\bar{u}_{\alpha,\beta}^o + M_{\alpha\beta}\delta\theta_{\alpha,\beta}} + N_{\alpha\beta}^h\delta\bar{u}_{\alpha,\beta}^h + M_{\alpha\beta}^h\delta\theta_{\alpha,\beta}^h + \underline{Q_\alpha\delta(\theta_\alpha + \bar{u}_{3,\alpha}^o)} + Q_\alpha^{(1)}\delta(2\bar{u}_\alpha^h) + Q_\alpha^{(2)}\delta(3\theta_\alpha^h) \tag{32}$$

and

$$\langle(\gamma_{\alpha 3} - S_{\alpha 3\beta 3}\sigma_{\beta 3})\delta\sigma_{\alpha 3}\rangle = 0, \tag{33}$$

where

$$\begin{Bmatrix} N_{\alpha\beta} \\ M_{\alpha\beta} \\ N_{\alpha\beta}^h \\ M_{\alpha\beta}^h \end{Bmatrix} = \begin{bmatrix} A_{\alpha\beta\gamma\omega} & B_{\alpha\beta\gamma\omega} & D_{\alpha\beta\gamma\omega} & H_{\alpha\beta\gamma\omega} \\ B_{\alpha\beta\gamma\omega} & D_{\alpha\beta\gamma\omega} & H_{\alpha\beta\gamma\omega} & A_{\alpha\beta\gamma\omega}^h \\ D_{\alpha\beta\gamma\omega} & H_{\alpha\beta\gamma\omega} & A_{\alpha\beta\gamma\omega}^h & B_{\alpha\beta\gamma\omega}^h \\ H_{\alpha\beta\gamma\omega} & A_{\alpha\beta\gamma\omega}^h & B_{\alpha\beta\gamma\omega}^h & D_{\alpha\beta\gamma\omega}^h \end{bmatrix} \begin{Bmatrix} \bar{\varepsilon}_{\gamma\omega}^o \\ \kappa_{\gamma\omega} \\ \varepsilon_{\gamma\omega}^h \\ \kappa_{\gamma\omega}^h \end{Bmatrix} \tag{34}$$

and

$$\begin{Bmatrix} Q_\alpha \\ Q_\alpha^{(1)} \\ Q_\alpha^{(2)} \end{Bmatrix} = \begin{bmatrix} \widehat{A}^{(0)}_{\alpha 3\beta 3} & \widehat{B}^{(0)}_{\alpha 3\beta 3} & \widehat{D}^{(0)}_{\alpha 3\beta 3} \\ \widehat{A}^{(1)}_{\alpha 3\beta 3} & \widehat{B}^{(1)}_{\alpha 3\beta 3} & \widehat{D}^{(1)}_{\alpha 3\beta 3} \\ \widehat{A}^{(2)}_{\alpha 3\beta 3} & \widehat{B}^{(2)}_{\alpha 3\beta 3} & \widehat{D}^{(2)}_{\alpha 3\beta 3} \end{bmatrix} \begin{Bmatrix} \phi_\beta \\ \zeta_\beta \\ \eta_\beta \end{Bmatrix}. \tag{35}$$

From Eq. (33), one can find that the transverse shear stresses variables can be expressed in terms of the displacement variables as follows:

$$\begin{Bmatrix} \phi_\beta \\ \zeta_\beta \\ \eta_\beta \end{Bmatrix} = \begin{bmatrix} \widetilde{A}_{\beta 3\gamma 3} & \widetilde{B}_{\beta 3\gamma 3} & \widetilde{E}_{\beta 3\gamma 3} \\ \widetilde{B}_{\beta 3\gamma 3} & \widetilde{D}_{\beta 3\gamma 3} & \widetilde{F}_{\beta 3\gamma 3} \\ \widetilde{E}_{\beta 3\gamma 3} & \widetilde{F}_{\beta 3\gamma 3} & \widetilde{A}^h_{\beta 3\gamma 3} \end{bmatrix}^{-1} \begin{bmatrix} \widehat{A}^{(0)}_{\gamma 3\lambda 3} & \widehat{B}^{(0)}_{\gamma 3\lambda 3} & \widehat{D}^{(0)}_{\gamma 3\lambda 3} \\ \widehat{A}^{(1)}_{\gamma 3\lambda 3} & \widehat{B}^{(1)}_{\gamma 3\lambda 3} & \widehat{D}^{(1)}_{\gamma 3\lambda 3} \\ \widehat{A}^{(2)}_{\gamma 3\lambda 3} & \widehat{B}^{(2)}_{\gamma 3\lambda 3} & \widehat{D}^{(2)}_{\gamma 3\lambda 3} \end{bmatrix}^{\mathrm{T}} \begin{Bmatrix} \bar{\gamma}_{\lambda 3} \\ 2\bar{u}^h_\lambda \\ 3\theta^h_\lambda \end{Bmatrix}, \tag{36}$$

where $\bar{\gamma}_{\lambda 3} \equiv \theta_\lambda + \bar{u}^o_{3,\lambda}$.

Substituting Eq. (36) into Eq. (35) yields

$$\begin{Bmatrix} Q_\alpha \\ Q_\alpha^{(1)} \\ Q_\alpha^{(2)} \end{Bmatrix} = \begin{bmatrix} \widehat{A}_{\alpha 3\beta 3} & \widehat{B}_{\alpha 3\beta 3} & \widehat{E}_{\alpha 3\beta 3} \\ \widehat{B}_{\alpha 3\beta 3} & \widehat{D}_{\alpha 3\beta 3} & \widehat{F}_{\alpha 3\beta 3} \\ \widehat{E}_{\alpha 3\beta 3} & \widehat{F}_{\alpha 3\beta 3} & \widehat{A}^h_{\alpha 3\beta 3} \end{bmatrix} \begin{Bmatrix} \bar{\gamma}_{\beta 3} \\ 2\bar{u}^h_\beta \\ 3\theta^h_\beta \end{Bmatrix}, \tag{37}$$

where the stiffness $\widehat{A}_{\alpha 3\beta 3}$ for EFSDT can be calculated by

$$\widehat{A}_{\alpha 3\beta 3} = \widehat{A}^{(0)}_{\alpha 3\lambda 3} \widetilde{A}^{-1}_{\lambda 3\gamma 3} \widehat{A}^{(0)}_{\gamma 3\beta 3}. \tag{38}$$

The stress resultants and stiffness matrices presented in Eqs. (34)–(36) are given in Appendix B.

4.1. Enhanced first-order shear deformation theory

Applying the variational principle of Eq. (15) according to Eqs. (31), (32), (34) and (37), the governing equations off the present EFSDT are given by

$$\begin{aligned} &\delta\bar{u}^o_\alpha : N_{\alpha\beta,\beta} = \ddot{N}^I_\alpha, \\ &\delta\theta_\alpha : M_{\alpha\beta,\beta} - Q_\alpha = \ddot{M}^I_\alpha, \\ &\delta\bar{u}^o_3 : Q_{\alpha,\alpha} = \ddot{V}^I_3, \end{aligned} \tag{39}$$

where

$$\begin{Bmatrix} \ddot{N}^I_\alpha \\ \ddot{M}^I_\alpha \\ \ddot{V}^I_3 \end{Bmatrix} = \begin{bmatrix} I^{(0)} & I^{(1)} & 0 \\ I^{(1)} & I^{(2)} & 0 \\ 0 & 0 & I^{(0)} \end{bmatrix} \begin{Bmatrix} \ddot{\bar{u}}^o_\alpha \\ \ddot{\theta}_\alpha \\ \ddot{\bar{u}}^o_3 \end{Bmatrix}, \quad I^{(j)} = \langle \rho x_3^j \rangle \quad (j = 0, 1, 2) \tag{40}$$

and associated boundary conditions are:

$$\begin{aligned} &\delta\bar{u}^o_\alpha = 0 \quad \text{or} \quad N_{\alpha\beta} v_\beta = 0, \\ &\delta\theta_\alpha = 0 \quad \text{or} \quad M_{\alpha\beta} v_\beta = 0, \\ &\delta\bar{u}^o_3 = 0 \quad \text{or} \quad Q_\alpha v_\alpha = 0, \end{aligned} \tag{41}$$

where v_α is the direction cosine to be projected on x_α axis.

Notice that the preceding equations present the governing equations of classical FSDT except the transverse shear force Q_α shown in Eq. (39).

It is important to accurately predict the through-the-thickness displacements that are the mode shapes in the case of elastodynamic problems. Higher-order zig-zag theories presented in the previous section can be used as

the post-processor to improve the prediction. This can be achieved by writing the displacement fields of higher-order zig-zag theories in terms of those of enhanced plate theories.

From the underline term presented in Eq. (26), one can obtain the following expression:

$$u_{\alpha,3} + u^o_{3,\alpha} = \mathscr{A}_{\alpha\beta}\phi_\beta, \tag{42}$$

which yields the following displacements of a third-order zig-zag plate theory for an EFSDT by integrating through the thickness:

$$u_\alpha = u^o_\alpha - u^o_{3,\alpha}x_3 + \Phi_{\alpha\beta}\phi_\beta, \quad u_3 = u^o_3, \tag{43}$$

where

$$\begin{aligned}\Phi_{\alpha\beta} &= \int \mathscr{A}_{\alpha\beta}\,\mathrm{d}x_3 \\ &= x_3\left(x_3^2 - \frac{3h^2}{4}\right)\delta_{\alpha\beta} + \sum_{k=1}^{N-1} a^{(k)}_{\alpha\beta}\left[-\frac{x_3}{h} - \frac{x_3^2}{2h} + (x_3 - x_{3(k)})H(x_3 - x_{3(k)})\right].\end{aligned} \tag{44}$$

The definition of the mean displacement through the thickness of the plate, $\bar{u}^o_i$, is given by

$$\bar{u}^o_i = \frac{1}{h}\langle u_i\rangle, \tag{45}$$

which leads to the kinematical constraints on the displacements given as

$$u^o_\alpha = \bar{u}^o_\alpha - \frac{1}{h}\langle\Phi_{\alpha\beta}\rangle\phi_\beta, \quad u^o_3 = \bar{u}^o_3. \tag{46}$$

Using Eqs. (36) and (46), one can recover the higher-order zig-zag displacement field as

$$u_\alpha = \bar{u}^o_\alpha - \bar{u}^o_{3,\alpha}x_3 + \left(\Phi_{\alpha\beta}\widetilde{A}^{-1}_{\beta3\gamma3}\widehat{A}^{(0)}_{\gamma3\lambda3} - \frac{1}{h}\langle\Phi_{\alpha\beta}\rangle\widetilde{A}^{-1}_{\beta3\gamma3}\widehat{A}^{(0)}_{\gamma3\lambda3}\right)\bar{\gamma}_{\lambda3}, \tag{47}$$

where $\bar{u}^o_i$ and $\bar{\gamma}_{\lambda3}$ can be obtained by solving Eq. (39).

4.2. Enhanced higher-order shear deformation theory

For an EHSDT, the same procedure presented in an EFSDT can be applied. After solving the governing equations of an EHSDT that are omitted here, one can recover the displacements of a fifth-order zig-zag plate theory. In other words, the variables in a fifth-order zig-zag theory can be expressed in terms of the variables of EHSDT ($\bar{u}_i$, θ_α, $\bar{u}^h_\alpha$ and θ^h_α).

From the whole term presented in Eq. (26), the shear strains of a fifth-order zig-zag plate theory can be expressed as

$$u_{\alpha,3} + u^o_{3,\alpha} = \mathscr{A}_{\alpha\beta}\phi_\beta + \mathscr{B}_{\alpha\beta}\zeta_\beta + \mathscr{C}_{\alpha\beta}\eta_\beta, \tag{48}$$

which yields

$$u_\alpha = u^o_\alpha - u^o_{3,\alpha}x_3 + \Phi_{\alpha\beta}\phi_\beta + \Phi^{(1)}_{\alpha\beta}\zeta_\beta + \Phi^{(2)}_{\alpha\beta}\eta_\beta, \quad u_3 = u^o_3, \tag{49}$$

where

$$\begin{aligned}\Phi^{(1)}_{\alpha\beta} &= \int \mathscr{B}_{\alpha\beta}\,\mathrm{d}x_3 \\ &= x_3^2\left(x_3^2 - \frac{h^2}{2}\right)\delta_{\alpha\beta} + \sum_{k=1}^{N-1} b^{(k)}_{\alpha\beta}\left[-\frac{x_3}{h} - \frac{x_3^2}{2h} + (x_3 - x_{3(k)})H(x_3 - x_{3(k)})\right],\end{aligned} \tag{50}$$

$$\Phi_{\alpha\beta}^{(2)} = \int \mathscr{C}_{\alpha\beta}\,\mathrm{d}x_3 = x_3\left(x_3^4 - \frac{5h^4}{16}\right)\delta_{\alpha\beta} + \sum_{k=1}^{N-1} c_{\alpha\beta}^{(k)}\left[-\frac{x_3}{h} - \frac{x_3^2}{2h} + (x_3 - x_{3(k)})H(x_3 - x_{3(k)})\right]. \tag{51}$$

The generalized definition of the mean displacement [41,42] can be written by

$$\left\langle \min_{\bar{u}_i^o}(u_i - \bar{u}_i)^2 \right\rangle = 0, \tag{52}$$

where u_i is from Eq. (49), and $\bar{u}_i$ from Eq. (31). This renders

$$u_\alpha^o = \bar{u}_\alpha^o + \frac{h^2}{12}\bar{u}_\alpha^h - \frac{1}{h}(\langle\Phi_{\alpha\beta}\rangle\phi_\beta + \langle\Phi_{\alpha\beta}^{(1)}\rangle\zeta_\beta + \langle\Phi_{\alpha\beta}^{(2)}\rangle\eta_\beta), \quad u_3^o = \bar{u}_3^o. \tag{53}$$

Using Eqs. (36) and (53), the higher-order zig-zag displacement given in Eq. (49) can be rewritten, in terms of the classical HSDT variables, as follows:

$$u_\alpha = \bar{u}_\alpha^o + \frac{h^2}{12}\bar{u}_\alpha^h - \bar{u}_{3,\alpha}^o x_3 + \left(\Phi_{\alpha\beta} - \frac{1}{h}\langle\Phi_{\alpha\beta}\rangle\right)\phi_\beta + \left(\Phi_{\alpha\beta}^{(1)} - \frac{1}{h}\langle\Phi_{\alpha\beta}^{(1)}\rangle\right)\zeta_\beta + \left(\Phi_{\alpha\beta}^{(2)} - \frac{1}{h}\langle\Phi_{\alpha\beta}^{(2)}\rangle\right)\eta_\beta, \tag{54}$$

where ϕ_β, ζ_β and η_β can be expressed in terms of $\bar{\gamma}_{\alpha 3}$, $\bar{u}_\alpha^h$ and θ_α^h using Eq. (36). The variables of EHSDT are obtained by solving the governing equations that are omitted here for the sake of brevity, since they are same as those of the classical HSDT except the stiffness related to the transverse shear forces.

5. Numerical examples and discussion

The accuracy of the present theories are assessed by presenting the analytical solutions for certain simply supported plates in cylindrical bending conditions. The exact solutions of elastodynamic problems developed by Chen and Lee [52] are reproduced and used as the benchmark solutions. For the present EFSDT, the displacements for simply supported edges can be chosen to be of the form:

$$[\bar{u}_\alpha^o, \theta_\alpha] = [U_\alpha, \Theta_\alpha]\cos\left(\frac{n\pi x_1}{L_1}\right)\cos(\omega t), \tag{55}$$

$$\bar{u}_3^o = U_3 \sin\left(\frac{n\pi x_1}{L_1}\right)\cos(\omega t), \tag{56}$$

which is for angle-ply lay-ups, whereas $\bar{u}_2^o = 0$ for cross-ply lay-ups. It is, however, convenient to use the same shape functions for both cross-ply and angle-ply lay-ups, since cross-ply lay-ups can be easily simulated by assuming the small angle perturbation, for example, $0^\circ \approx 0.001^\circ$ and $90^\circ \approx 90.001^\circ$. For EHSDT, $\bar{u}_\alpha^h$ and θ_α^h have the same form presented in Eq. (55).

Several examples of lamination angle and stacking sequence for laminated and sandwich plates are considered for comparison. Material properties used in this study are given in Table 1. Normalized frequencies reported in figures and tables are defined by

$$\bar{\omega} = \omega h\sqrt{\frac{\rho}{G_{12}}}, \tag{57}$$

where ρ indicates the material density, and G_{12} represents the material property of the orthotropic ply.

The percentage error of frequency is also presented to provide the qualitative behavior, which is given by

$$e\% = \frac{(\bar{\omega} - \bar{\omega}_{3D})}{\bar{\omega}_{3D}} \times 100, \tag{58}$$

where a negative value indicates an underestimation with respect to the exact 3D results.

The various models compared in the present study are listed in Table 2. A SCF is not considered in the FSDT. In this study, the FSDT and HSDT results are reproduced, while the PAR and M2D results are taken

Table 1
Material properties for laminated and sandwich plates

	Ply and face sheet	Core material [53]
E_{11}	25×10^6 psi (172.4 GPa)	0.145×10^5 psi (0.1 GPa)
E_{22}	1×10^6 psi (6.9 GPa)	0.145×10^5 psi (0.1 GPa)
E_{33}	1×10^6 psi (6.9 GPa)	0.145×10^5 psi (0.1 GPa)
v_{12}	0.25	0.25
v_{23}	0.25	0.25
v_{13}	0.25	0.25
G_{12}	0.5×10^6 psi (3.45 GPa)	0.58×10^4 psi (0.04 GPa)
G_{23}	0.2×10^6 psi (1.38 GPa)	0.58×10^4 psi (0.04 GPa)
G_{13}	0.5×10^6 psi (3.45 GPa)	0.58×10^4 psi (0.04 GPa)

Table 2
Shear deformation plate theories compared

Source	Theory	Degrees of freedom
Present	EFSDT	5
Present	EHSDT	9
Whitney–Pagano [5]	FSDT	5
Pandya–Kant [13,15]	HSDT	9
Timarci–Soldatos [14]	PAR	5
Messina [49]	M2D3, M2D7	9, 17

from Ref. [49]. A graphical representation of displacements and transverse shear stresses reported herein are scaled by the displacement at the bottom surface, $u_1(-h/2)$, so that the results predicted by the different models can be compared.

5.1. Summary of the present EFSDT and EHSDT

The overall procedure for the present EFSDT and EHSDT can be summarized as follows:

- Assume the transverse shear stresses of Eq. (30) from the third-order (for EFSDT) or fifth-order (for EHSDT) zig-zag plate theories.
- Assume the displacements of Eq. (31) from the classical FSDT and HSDT.
- Formulate the equations by substituting both assumed displacements and transverse shear stresses into the mixed variational theorem.
- Solve the constraint equations presented in Eq. (33) to find the relationships, Eq. (36), between FSDT (or HSDT) and third-order (or fifth-order) zig-zag plate theory.
- Obtain the governing equations, e.g. Eq. (39) for EFSDT, that are the same as those of FSDT and HSDT except the stiffness related to the transverse shear forces.
- Solve the governing equations, e.g. Eq. (39) for EFSDT, by substituting spatial shape functions, e.g. Eqs. (55) and (56) for EFSDT, to find the natural frequencies (ω) and corresponding mode shapes ($\bar{u}_i^o$ and θ_α for EFSDT; $\bar{u}_i^o$, θ_α, $\bar{u}_\alpha^h$ and θ_α^h for EHSDT, which are referred to as the base solutions in this paper).
- Recover the displacements u_α of Eqs. (47) and (54) and the transverse shear stresses $\sigma_{\alpha 3}$ of Eq. (30) via Eq. (36) using the base solutions of EFSDT and EHSDT.

As mentioned above, the present EFSDT and EHSDT enhance the prediction of global behavior of the plate by modifying the transverse shear stiffness via the mixed variational theorem as compared to the classical FSDT and HSDT, and improve the local through-the-thickness distributions of displacements and stresses by recovering to those of higher-order zig-zag theories (third-order for EFSDT and fifth-order for EHSDT).

Numerical results reported in tables and figures are obtained by solving the governing equations for natural frequencies ω, and by post-processing the base solutions using higher-order zig-zag theories for displacements u_α, Eqs. (47) and (54), and transverse shear stresses $\sigma_{\alpha 3}$, Eq. (30) via Eq. (36). The first derivatives with respect to in-plane coordinates x_α are only needed for the recovered displacements and transverse shear stresses presented herein, which confirms the numerical efficiency of the present models. All the results of 3D exact, FSDT, and HSDT presented in tables and figures are reproduced in this paper.

5.2. Laminated composite plates

Tables 3 and 4 compare normalized first thickness frequencies of cross-ply and angle-ply plates, respectively, for the length-to-thickness ratio, $L_1/h = 10$, and the wavenumber, $n = 1$. It can be seen that the present EFSDT and EHSDT models yield always better predictions than the classical FSDT and HSDT with the same computational efforts. The present EFSDT yields comparable results with the PAR_{cs} and PAR_{ds} that are based on cubic higher-order theories. In most cases, the present EHSDT can produce accurate results as the M2D3 and M2D7 that are constructed using fifth- and ninth-order polynomials, respectively, can do. For anti-symmetric plates ($[0^\circ/90^\circ]_s$ and $[45^\circ/-45^\circ]_s$), the EHSDT shows slightly underpredicts as compared to the M2D3 and M2D7. With increasing the number of layers, however, the EHSDT does provide better results. As was discussed in Ref. [49], the fulfillment of the transverse shear stresses continuity requirements and the accurate simulation of kinky displacement distributions attribute to this. For instance, the mode shapes and transverse shear stresses of a $[(0^\circ/90^\circ)_3/0^\circ]_s$ plate for $L_1/h = 10$ and $n = 3$ are shown and compared with the 3D results in Fig. 2.

Table 3
Normalized first frequencies, $\bar{\omega}$, for cross-ply plates ($L_1/h = 10; n = 1$)

	$[0^\circ/90^\circ/0^\circ]$	$e\%$	$[0^\circ/90^\circ]_2$	$e\%$	$[(0^\circ/90^\circ)_3/0^\circ]_s$	$e\%$
3D	0.146248	–	0.109461	–	0.129758	–
EFSDT	0.144788	−1.00	0.112513	2.79	0.129139	−0.48
EHSDT	0.146027	−0.15	0.109081	−0.35	0.129760	0.00
FSDT	0.161610	10.50	0.118552	8.30	0.137052	5.62
HSDT	0.150482	2.89	0.113871	4.03	0.134079	3.33
PAR_{cs}	0.146384	0.09	0.112403	2.69	0.129924	0.13
PAR_{ds}	0.151077	3.30	0.115672	5.67	0.134168	3.40
M2D3	0.145844	−0.28	0.109150	−0.28	0.129739	−0.01
M2D7	0.146210	−0.03	0.109239	−0.20	0.129808	0.04

Table 4
Normalized first frequencies, $\bar{\omega}$, for angle-ply plates ($L_1/h = 10; n = 1$)

	$[45^\circ/-45^\circ/45^\circ]$	$e\%$	$[45^\circ/-45^\circ]_2$	$e\%$	$[(45^\circ/-45^\circ)_3/45^\circ]_s$	$e\%$
3D	0.0911137	–	0.0883295	–	0.0959047	–
EFSDT	0.0907351	−0.42	0.0896349	1.48	0.0959147	0.01
EHSDT	0.0910117	−0.11	0.0881841	−0.16	0.0958936	−0.01
FSDT	0.0966205	6.04	0.0925953	4.83	0.0991789	3.41
HSDT	0.0927193	1.76	0.0905042	2.46	0.0977394	1.91
PAR_{cs}	0.0911503	0.04	0.0895849	1.42	0.0959541	0.05
PAR_{ds}	0.0929594	2.03	0.0912185	3.27	0.0977788	1.95
M2D3	0.0909154	−0.22	0.0882111	−0.13	0.0958935	−0.01
M2D7	0.0910817	−0.04	0.0882121	−0.13	0.0959152	0.01

In Fig. 3, the fifth thickness mode shapes and corresponding transverse shear stresses are presented and compared with the 3D exact solutions for an anti-symmetric cross-ply plate of $[0^\circ/90^\circ]_s$ with $L_1/h = 10$ and $n = 1$. In this case, it is easy to see the advantages of the EFSDT and EHSDT against the classical FSDT and HSDT. The present models are far better than the classical FSDT and HSDT in terms of both the mode shapes and transverse shear stresses. Especially, the fifth thickness mode shapes predicted by the 3D elasticity approach and the present EHSDT are indistinguishable in practice.

Results of the first thickness mode for the thick anti-symmetric angle-ply plate of $[45^\circ/-45^\circ]_s$ ($L_1/h = 4$, $n = 1$) are shown in Fig. 4 showing the distributions of displacement u_2 and transverse shear stress σ_{23} due to the transverse shear coupling. As shown in Fig. 4, even the present EFSDT, which is the counterpart of the classical FSDT, can qualitatively predict kinky displacement and transverse shear stress distributions. In fact, the EFSDT is more accurate than both the classical FSDT and HSDT in predicting the fundamental frequency.

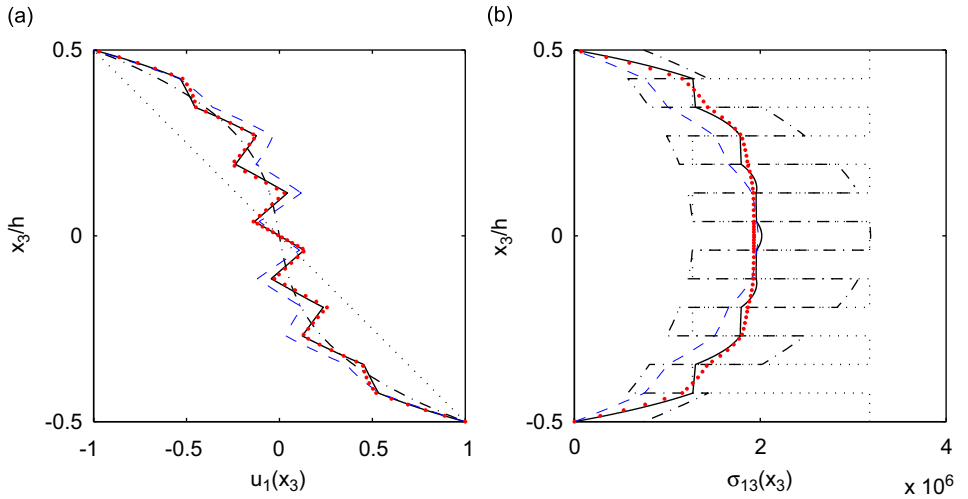

Fig. 2. First thickness mode shapes of a $[(0^\circ/90^\circ)_3/0^\circ]_s$ plate ($L_1/h = 10, n = 3$): (a) u_1; (b) σ_{13}; —: 3D (0.611978), — —: EFSDT (0.59819, −2.25%), ●: EHSDT (0.61057, −0.23%), ···: FSDT (0.69897, 14.2%), — · —: HSDT (0.664929, 8.66%).

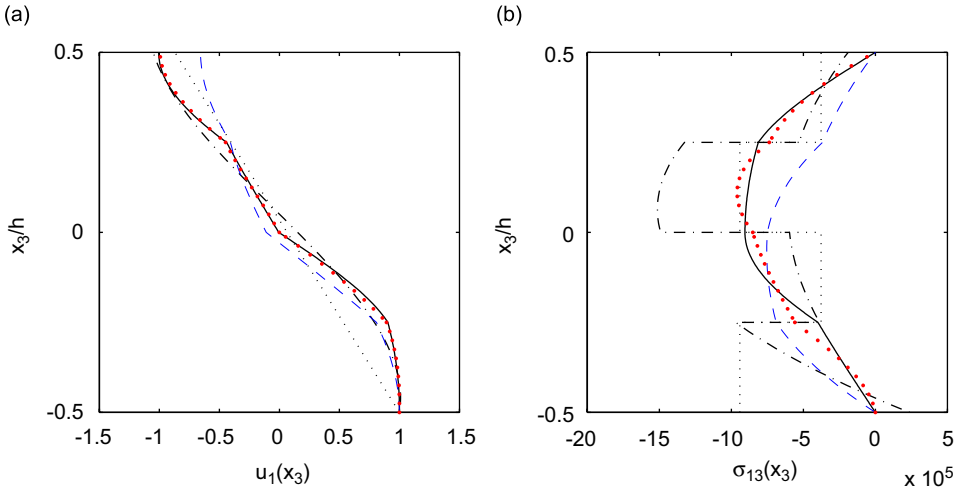

Fig. 3. Fifth thickness mode shapes of a $[0^\circ/90^\circ]_2$ plate ($L_1/h = 10, n = 1$): (a) u_1; (b) σ_{13}; —: 3D (2.869107), — —: EFSDT (2.868259, −0.03%), ●: EHSDT (2.903368, 1.19%), ···: FSDT (3.338892, 16.4%), — · —: HSDT (3.079155, 7.3%).

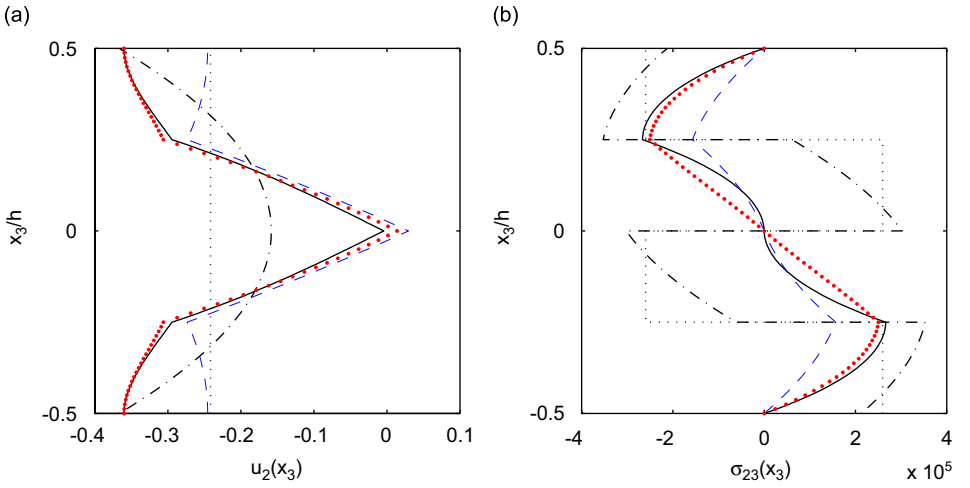

Fig. 4. First thickness mode shapes of a $[45^\circ/-45^\circ]_2$ plate ($L_1/h = 4, n = 1$): (a) u_2; (b) σ_{23}; —: 3D (0.387295), — —: EFSDT (0.4004, 3.38%), ●: EHSDT (0.382803, −1.16%), ···: FSDT (0.513709, 32.6%), — · —: HSDT (0.413884, 6.87%).

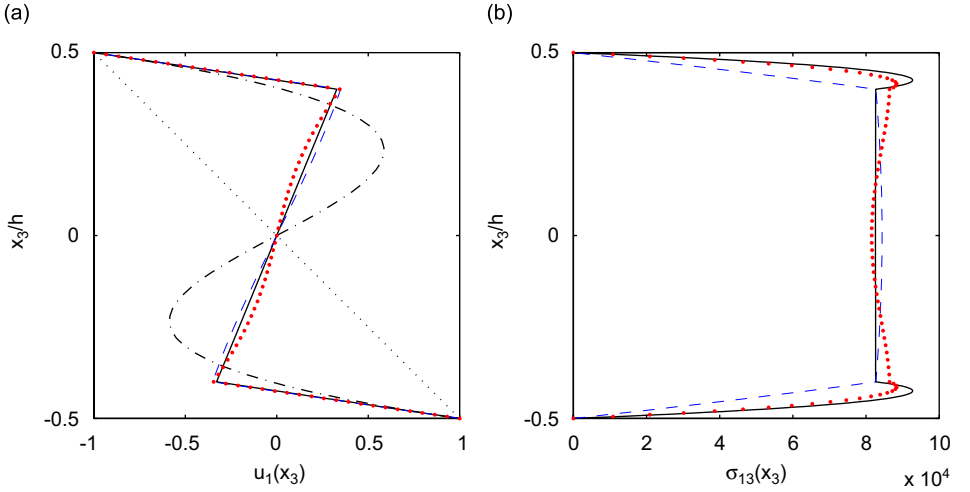

Fig. 5. First thickness mode shapes of a $[0^\circ/\text{core}/0^\circ]$ plate ($L_1/h = 10, n = 1$); reference Tables 5 and 6: (a) u_1; (b) σ_{13}; —: 3D, — —: EFSDT, ●: EHSDT, ···: FSDT, — · —: HSDT.

5.3. Sandwich plates

In this subsection, the present EFSDT and EHSDT are applied to a very challenging problem of the sandwich plate. The first thickness mode of a sandwich plate ($[0^\circ/\text{core}/0^\circ]$) with $L_1/h = 10$ and $n = 1$ is a pure bending one as shown in Fig. 5. Displacement u_1 and transverse shear stress σ_{13} distributions indicate that they can be well represented by the present EFSDT and EHSDT, whereas the classical HSDT shows a severe distortion of the displacement u_1 in the elastic core. Transverse shear stresses calculated by the classical FSDT and HSDT are omitted in Fig. 5, since they are far away from the 3D prediction.

Table 5 compare the results obtained by the EFSDT, EHSDT and HSDT for the first thickness frequencies of a $[0^\circ/\text{core}/0^\circ]$ plate with increasing the wave number, $n = 1$–5, and fixed length-to-thickness ratio, $L_1/h = 50$. As clearly shown in Table 5, both the EFSDT and EHSDT show an excellent agreement with the 3D results. Maximum percentage error of the EFSDT is −3.2%, while the classical HSDT produces 25% error.

Table 6 lists the first five thickness frequencies with increasing the length-to-thickness ratio, $L_1/h = 4$–200, and $n = 1$, for the same sandwich plate. As expected, the first thickness frequencies get closer to the 3D results, as the length-to-thickness L_1/h increases. An exception is provided with the fourth and fifth thickness modes where a large discrepancy is presented in the present EFSDT (10.7%) and the classical FSDT (357.1%). In particular, the errors of the FSDT are significant (more than 300%, see values with boldface in Table 6), since the classical FSDT cannot represent characteristic of the sandwich behavior. It is observed that the fourth and fifth thickness modes are dominated by the deformation of the core, whereas the first three modes (one bending and two membrane modes) are global [54]. In fact, the fourth and fifth modes can be interpreted as the transverse shear modes of the sandwich core. This is clearly shown in Fig. 6 that shows the fifth thickness mode shapes and corresponding transverse shear stresses. The classical FSDT cannot distinguish the difference between global bending and core shear modes.

The transverse shear stresses of an anti-symmetric sandwich plate ([45°/core/ − 45°]) are presented in Fig. 7 for $L_1/h = 10$ and $n = 1$. As it can be seen in this figure, the present enhance plate theories agree well with the 3D exact solutions (frequency error is less than 0.3%). For the transverse shear stress σ_{23}, however, the present theories are not evidently able to provide accurate predictions (highly localized distributions) for the limitation of an equivalent single layer theory. In such cases, the equilibrium approach for the evaluation of transverse shear stresses could help to improve predictions, since the displacement distributions (in-plane strains) are accurately predicted by the present theory.

Table 5
Normalized first frequencies, $\bar{\omega}$, for a sandwich plate ([0°/core/0°]; $L_1/h = 50$)

n	Exact 3D	EFSDT	e%	EHSDT	e%	HSDT	e%
1	0.004351	0.0043461	−0.1	0.0043529	0.0	0.0047519	9.2
2	0.011735	0.0116749	−0.5	0.0117354	0.0	0.0139243	18.7
3	0.019209	0.0189828	−1.2	0.0191854	−0.1	0.0235972	22.8
4	0.026680	0.0261231	−2.1	0.0265960	−0.3	0.0332176	24.5
5	0.034263	0.0331583	−3.2	0.0340682	−0.6	0.0428328	25.0

Table 6
Normalized frequencies, $\bar{\omega}$, for a sandwich plate ([0°/core/0°]; $n = 1$)

$\frac{L_1}{h}$	No.	3D	EFSDT	e%	EHSDT	e%	FSDT	e%
4	1	0.101069	0.084893	−16.0	0.097208	−3.8	0.332518	229.0
10	1	0.034263	0.033158	−3.2	0.034068	−0.6	0.100527	193.4
20	1	0.015479	0.015353	−0.8	0.015471	−0.0	0.031619	104.3
50	1	0.004351	0.004346	−0.1	0.004353	0.0	0.005532	27.1
	2	0.028705	0.028744	0.1	0.028716	0.0	0.028744	0.1
	3	0.185298	0.199186	7.5	0.193189	4.3	0.199186	7.5
	4	0.342624	0.377629	10.2	0.338485	−1.2	1.036007	**202.4**
	5	0.430430	0.488030	13.4	0.430683	0.1	1.615174	**275.2**
100	1	0.001303	0.001303	−0.0	0.001303	0.0	0.001403	7.7
	2	0.014367	0.014372	0.0	0.014368	0.0	0.014372	0.0
	3	0.097797	0.099593	1.8	0.098828	1.1	0.099593	1.8
	4	0.340988	0.375688	10.2	0.336774	−1.2	1.035301	**204.6**
	5	0.366099	0.407041	11.2	0.359696	−1.7	1.592395	**335.0**
200	1	0.000345	0.000345	0.0	0.000345	0.0	0.000352	2.0
	2	0.007185	0.007186	0.0	0.007186	0.0	0.007186	0.0
	3	0.049570	0.049797	0.5	0.049700	0.3	0.049797	0.5
	4	0.340578	0.375201	10.2	0.336345	−1.2	1.035124	**203.9**
	5	0.347129	0.384131	10.7	0.339581	−2.2	1.586648	**357.1**

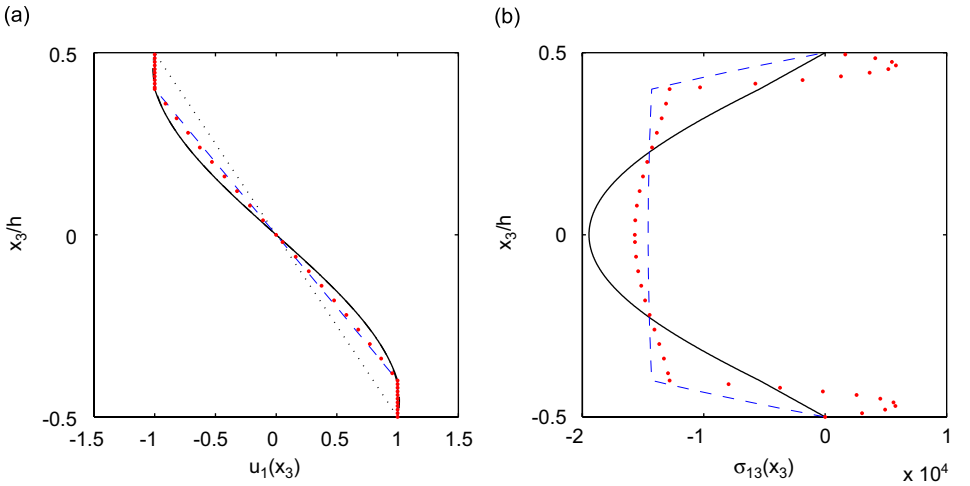

Fig. 6. Fifth thickness mode shapes of a $[0^\circ/\text{core}/0^\circ]$ plate ($L_1/h = 200, n = 1$); reference Tables 5 and 6: (a) u_1; (b) σ_{13}; —: 3D, – –: EFSDT, ●: EHSDT, ···: FSDT, — · —: HSDT.

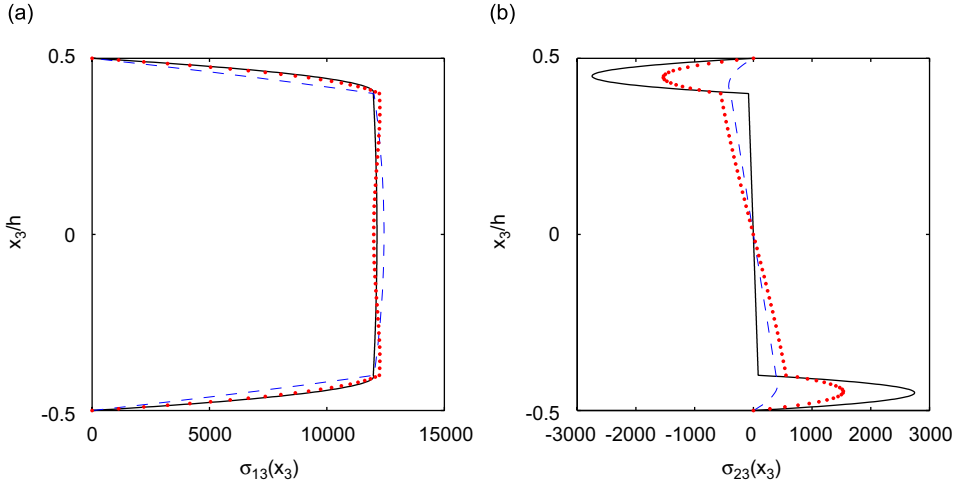

Fig. 7. Transverse shear stresses of a $[45^\circ/\text{core}/-45^\circ]$ plate corresponding to the first thickness mode ($L_1/h = 10, n = 1$): (a) σ_{13}; (b) σ_{23}; —: 3D (0.024638), – –: EFSDT (0.024322, −0.88%), ●: EHSDT (0.024589, 0.21%), ···: FSDT (0.033205, 35.3%), — · —: HSDT (0.026828, 9.33%).

6. Conclusions

Two enhanced plate theories for laminated and sandwich plates are developed via the mixed variational formulation for free vibration studies. By obtaining the transverse shear stresses based on higher-order zig-zag theories, the mixed variational formulation embraces them as the classical FSDT and HSDT, which renders the present enhanced plate theories (EFSDT and EHSDT). The obtained transverse shear stresses satisfy the continuity condition at the interface and stress free conditions on the top and bottom surfaces. Relationships between the higher-order zig-zag theories and the classical FSDT and HSDT are systematically derived via the mixed variational theorem and the generalized definition of the mean displacement [41,42].

The present theories are used to explore the thickness modes of laminated and sandwich plates. Comparisons of mode shapes and transverse shear stresses for laminated and sandwich plates are made with the available data reported in literature and 3D exact solutions. Although resulting enhanced plate theories are as simple as equivalent single layer theories, FSDT and HSDT, the recovered results such as displacements

and transverse shear stresses have excellent accuracy as compared to the classical shear deformation theories (FSDT and HSDT) and other higher-order theories (PAR and M2D3).

Appendix A. Transverse shear stress continuity conditions

The continuity conditions of transverse shear stresses given in Eq. (24) are expressed of the matrix form:

$$[K]\{S\} = \{A_1\}\phi_1 + \{A_2\}\phi_2 + \{B_1\}\zeta_1 + \{B_2\}\zeta_2 + \{C_1\}\eta_1 + \{C_2\}\eta_2, \tag{A.1}$$

where

$$\{S\} = \lfloor S_1^{(1)} \cdots S_1^{(N-1)} \;\; S_2^{(1)} \cdots S_2^{(N-1)} \rfloor^{\mathrm{T}}. \tag{A.2}$$

Components of $[K]$ are computed by the following algorithm:

for $i = 1 : (N-1)$
  for $j = 1 : (i-1)$
    $K(i,j) = (C_{2313}^{(i+1)} - C_{2313}^{(i)})(x_{3(i)}/h + 1/2 - 1)$
    $K(i, N-1+j) = (C_{2323}^{(i+1)} - C_{2323}^{(i)})(x_{3(i)}/h + 1/2 - 1)$
    $K(N-1+i,j) = (C_{1313}^{(i+1)} - C_{1313}^{(i)})(x_{3(i)}/h + 1/2 - 1)$
    $K(N-1+i, N-1+j) = (C_{1323}^{(i+1)} - C_{1323}^{(i)})(x_{3(i)}/h + 1/2 - 1)$
  end
  for $j = (i+1) : (N-1)$
    $K(i,j) = (C_{2313}^{(i+1)} - C_{2313}^{(i)})(x_{3(i)}/h + 1/2)$
    $K(i, N-1+j) = (C_{2323}^{(i+1)} - C_{2323}^{(i)})(x_{3(i)}/h + 1/2)$
    $K(N-1+i,j) = (C_{1313}^{(i+1)} - C_{1313}^{(i)})(x_{3(i)}/h + 1/2)$
    $K(N-1+i, N-1+j) = (C_{1323}^{(i+1)} - C_{1323}^{(i)})(x_{3(i)}/h + 1/2)$
  end
  $K(i,i) = C_{2313}^{(i+1)}(x_{3(i)}/h + 1/2 - 1) - C_{2313}^{(i)}(x_{3(i)}/h + 1/2)$
  $K(i, N-1+i) = C_{2323}^{(i+1)}(x_{3(i)}/h + 1/2 - 1) - C_{2323}^{(i)}(x_{3(i)}/h + 1/2)$
  $K(N-1+i,i) = C_{1313}^{(i+1)}(x_{3(i)}/h + 1/2 - 1) - C_{1313}^{(i)}(x_{3(i)}/h + 1/2)$
  $K(N-1+i, N-1+i) = C_{1323}^{(i+1)}(x_{3(i)}/h + 1/2 - 1) - C_{1323}^{(i)}(x_{3(i)}/h + 1/2)$
end

Components of $\{A_\alpha\}$, $\{B_\alpha\}$ and $\{C_\alpha\}$ are computed as:

for $i = 1 : (N-1)$
  $A_1(i) = 3(x_{3(i)}^2 - h^2/4)(C_{2313}^{(i+1)} - C_{2313}^{(i)})$
  $A_1(N-1+i) = 3(x_{3(i)}^2 - h^2/4)(C_{1313}^{(i+1)} - C_{1313}^{(i)})$
  $A_2(i) = 3(x_{3(i)}^2 - h^2/4)(C_{2323}^{(i+1)} - C_{2323}^{(i)})$
  $A_2(N-1+i) = 3(x_{3(i)}^2 - h^2/4)(C_{2313}^{(i+1)} - C_{2313}^{(i)})$

  $B_1(i) = 4x_{3(i)}(x_{3(i)}^2 - h^2/4)(C_{2313}^{(i+1)} - C_{2313}^{(i)})$
  $B_1(N-1+i) = 4x_{3(i)}(x_{3(i)}^2 - h^2/4)(C_{1313}^{(i+1)} - C_{1313}^{(i)})$
  $B_2(i) = 4x_{3(i)}(x_{3(i)}^2 - h^2/4)(C_{2323}^{(i+1)} - C_{2323}^{(i)})$
  $B_2(N-1+i) = 4x_{3(i)}(x_{3(i)}^2 - h^2/4)(C_{2313}^{(i+1)} - C_{2313}^{(i)})$

  $C_1(i) = 5(x_{3(i)}^4 - h^4/16)(C_{2313}^{(i+1)} - C_{2313}^{(i)})$
  $C_1(N-1+i) = 5(x_{3(i)}^4 - h^4/16)(C_{1313}^{(i+1)} - C_{1313}^{(i)})$
  $C_2(i) = 5(x_{3(i)}^4 - h^4/16)(C_{2323}^{(i+1)} - C_{2323}^{(i)})$

$C_2(N-1+i) = 5(x_{3(i)}^4 - h^4/16)(C_{2313}^{(i+1)} - C_{2313}^{(i)})$

end

Thus the change in slope at each interface, $S_\alpha^{(k)}$, is expressed by

$$S_\alpha^{(k)} = a_{\alpha\beta}^{(k)}\phi_\beta + b_{\alpha\beta}^{(k)}\zeta_\beta + c_{\alpha\beta}^{(k)}\eta_\beta \quad (k = 1, \ldots, N-1), \tag{A.3}$$

where $a_{11}^{(k)}$ represents kth row of $[K]^{-1}\{A_1\}$, $a_{21}^{(k)}$ is $(N-1+k)$th row of $[K]^{-1}\{A_1\}$, $a_{12}^{(k)}$ is kth row of $[K]^{-1}\{A_2\}$, and $a_{22}^{(k)}$ is $(N-1+k)$th row of $[K]^{-1}\{A_2\}$. The computation of $b_{\alpha\beta}^{(k)}$ (components of $[K]^{-1}\{B_\alpha\}$) and $c_{\alpha\beta}^{(k)}$ (components of $[K]^{-1}\{C_\alpha\}$) is similar to that of $a_{\alpha\beta}^{(k)}$.

Appendix B. Definitions of the resultants and stiffness

Stress resultants and stiffness given in Eqs. (34) and (35) are defined by

$$[N_{\alpha\beta}, M_{\alpha\beta}, N_{\alpha\beta}^h, M_{\alpha\beta}^h] = \langle \sigma_{\alpha\beta}^{2D}[1, x_3, x_3^2, x_3^3]\rangle, \tag{B.1}$$

$$[Q_\alpha, Q_\alpha^{(1)}, Q_\alpha^{(2)}] = \langle \sigma_{\alpha 3}[1, x_3, x_3^2]\rangle, \tag{B.2}$$

$$[A_{\alpha\beta\gamma\omega}, B_{\alpha\beta\gamma\omega}, D_{\alpha\beta\gamma\omega}, H_{\alpha\beta\gamma\omega}] = \langle Q_{\alpha\beta\gamma\omega}[1, x_3, x_3^2, x_3^3]\rangle, \tag{B.3}$$

$$[A_{\alpha\beta\gamma\omega}^h, B_{\alpha\beta\gamma\omega}^h, D_{\alpha\beta\gamma\omega}^h] = \langle Q_{\alpha\beta\gamma\omega}[x_3^4, x_3^5, x_3^6]\rangle, \tag{B.4}$$

$$\widehat{A}_{\alpha 3\beta 3}^{(i)} = \langle x_3^i C_{\alpha 3\gamma 3}\mathscr{A}_{\gamma\beta}\rangle \quad (i = 0, 1, 2), \tag{B.5}$$

$$\widehat{B}_{\alpha 3\beta 3}^{(i)} = \langle x_3^i C_{\alpha 3\gamma 3}\mathscr{B}_{\gamma\beta}\rangle \quad (i = 0, 1, 2), \tag{B.6}$$

$$\widehat{D}_{\alpha 3\beta 3}^{(i)} = \langle x_3^i C_{\alpha 3\gamma 3}\mathscr{C}_{\gamma\beta}\rangle \quad (i = 0, 1, 2), \tag{B.7}$$

$$\widetilde{A}_{\beta 3\gamma 3} = \langle \mathscr{A}_{\beta\lambda} C_{\lambda 3\mu 3}\mathscr{A}_{\mu\gamma}\rangle, \quad \widetilde{B}_{\beta 3\gamma 3} = \langle \mathscr{A}_{\beta\lambda} C_{\lambda 3\mu 3}\mathscr{B}_{\mu\gamma}\rangle, \tag{B.8}$$

$$\widetilde{E}_{\beta 3\gamma 3} = \langle \mathscr{A}_{\beta\lambda} C_{\lambda 3\mu 3}\mathscr{C}_{\mu\gamma}\rangle, \quad \widetilde{D}_{\beta 3\gamma 3} = \langle \mathscr{B}_{\beta\lambda} C_{\lambda 3\mu 3}\mathscr{B}_{\mu\gamma}\rangle, \tag{B.9}$$

$$\widetilde{F}_{\beta 3\gamma 3} = \langle \mathscr{B}_{\beta\lambda} C_{\lambda 3\mu 3}\mathscr{C}_{\mu\gamma}\rangle, \quad \widetilde{A}_{\beta 3\gamma 3}^h = \langle \mathscr{C}_{\beta\lambda} C_{\lambda 3\mu 3}\mathscr{C}_{\mu\gamma}\rangle. \tag{B.10}$$

References

[1] E. Reissner, The effect of transverse shear deformation on the bending of elastic plates, *Journal of Applied Mechanics* 12 (1945) 69–77.
[2] E. Reissner, On a variational theorem in elasticity, *Journal of Mathematics and Physics* 29 (1950) 90–95.
[3] R.D. Mindlin, Influence of rotary inertia and shear on flexural motions of isotropic, elastic plates, *Journal of Applied Mechanics* 18 (1951) 31–38.
[4] P.C. Yang, C.H. Norris, Y. Stavsky, Elastic wave propagation in heterogeneous plates, *International Journal of Solids and Structures* 2 (1966) 665–684.
[5] J.M. Whitney, N.J. Pagano, Shear deformation in heterogeneous anisotropic plates, *Journal of Applied Mechanics* 37 (1970) 1031–1036.
[6] C.T. Sun, J.M. Whitney, Theories for the dynamic response of laminated plates, *AIAA Journal* 11 (1973) 178–183.
[7] J.N. Reddy, Free vibration of antisymmetric angle ply laminated plates including transverse shear deformation by the finite element method, *Journal of Sound and Vibration* 4 (1979) 565–576.
[8] K.M. Liew, Y. Xiang, S. Kitipornchai, Research on thick plate vibration: a literature survey, *Journal of Sound and Vibration* 180 (1995) 163–176.
[9] K.H. Lo, R.M. Christensen, F.M. Wu, A higher-order theory of plate deformation, part 2: laminated plates, *Journal of Applied Mechanics* 44 (1977) 669–676.

[10] M. Levinson, An accurate simple theory of the statics and dynamics of elastic plates, *Mechanics Research Communications* 7 (1980) 343–350.
[11] T. Kant, Numerical analysis of thick plates, *Computer Methods in Applied Mechanics and Engineering* 31 (1982) 1–18.
[12] J.N. Reddy, A simple higher-order theory for laminated composite plates, *Journal of Applied Mechanics* 51 (1984) 745–752.
[13] B.N. Pandya, T. Kant, Finite element stress analysis of laminated composite plates using higher order displacement model, *Composites Science and Technology* 32 (1988) 137–155.
[14] T. Timarci, K.P. Soldatos, Comparative dynamic studies for symmetric cross-ply circular cylindrical shells on the basis of a unified shear deformable shell theory, *Journal of Sound and Vibration* 187 (1995) 609–624.
[15] T. Kant, K. Swaminatha, Analytical solutions for free vibration of laminated composite and sandwich plates based on a higher-order refined theory, *Composite Structures* 53 (2001) 73–85.
[16] J.N. Reddy, A generalization of two-dimensional theories of laminated plates, *Communication in Numerical Methods in Engineering* 3 (1987) 173–180.
[17] K.N. Cho, C.W. Bert, A.G. Striz, Free vibrations of laminated rectangular plates analyzed by higher-order individual-layer theory, *Journal of Sound and Vibration* 145 (1991) 429–442.
[18] A. Nosier, R.K. Kapania, J.N. Reddy, Free vibration analysis of laminated plates using a layer-wise theory, *AIAA Journal* 31 (1993) 2335–2346.
[19] Y.Y. Yu, A new theory of elastic sandwich plates—one dimensional case, *ASME: Journal of Applied Mechanics* 26 (1959) 415–421.
[20] M. DiSciuva, Vibration and buckling of simply supported thick multilayered orthotropic plates: an evaluation of a new displacement model, *Journal of Sound and Vibration* 105 (1986) 425–442.
[21] M. Cho, R.R. Parmerter, An efficient higher order plate theory for laminated composites, *Composite Structures* 20 (1992) 113–123.
[22] M. Cho, R.R. Parmerter, Efficient higher order composite plate theory for general lamination configurations, *AIAA Journal* 31 (1993) 1299–1306.
[23] M. DiSciuva, Multilayered anisotropic plate models with continuous interlaminar stresses, *Composite Structures* 22 (1992) 149–167.
[24] M. DiSciuva, A general quadrilateral multilayered plate element with continuous interlaminar stresses, *Computers and Structures* 47 (1993) 91–105.
[25] E. Carrera, Historical review of zig-zag theories for multilayered plates and shells, *Applied Mechanics Review* 56 (2003) 287–308.
[26] J.M. Whitney, Stress analysis of thick laminated composites and sandwich plates, *Journal of Composite Materials* 6 (1972) 426–440.
[27] J.M. Whitney, Shear correction factors for orthotropic laminates under static load, *Journal of Applied Mechanics* 40 (1973) 302–304.
[28] A.K. Noor, W.S. Burton, Stress and free vibration analysis of multilayered composite plates, *Composite Structures* 14 (1990) 233–265.
[29] M. Cho, J.H. Kim, Postprocess method using displacement field of higher order laminated composite plate theory, *AIAA Journal* 34 (1996) 362–368.
[30] M. Cho, Y.J. Choi, A new postprocessing method for laminated composites of general lamination configurations, *Composite Structures* 54 (2001) 397–406.
[31] J.-S. Kim, M. Cho, Matching technique of postprocess method using displacement fields of higher order plate theories, *Composite Structures* 43 (1998) 71–78.
[32] M. Cho, J.-S. Kim, Four-noded finite element post-process method using a displacement filed of higher order laminated composite plate theory, *Computers and Structures* 61 (1996) 283–290.
[33] M. Cho, J.-S. Kim, Improved mindlin plate stress analysis for laminated composites in finite element method, *AIAA Journal* 35 (1997) 587–590.
[34] Y. Qi, N.F. Knight Jr., A refined first-order shear-deformation theory and its justification by plate-strain bending problem of laminated plates, *International Journal of Solids and Structures* 33 (1996) 49–64.
[35] N.F. Knight Jr., Y. Qi, Restatement of first-order shear-deformation theory for laminated plates, *International Journal of Solids and Structures* 34 (1997) 49–64.
[36] V.L. Berdichevsky, Variational-asymptotic method of construction a theory of shell, *Applied Mathematics and Mechanics (PMM)* 43 (1979) 664–687.
[37] V.G. Sutyrin, Derivation of plate theory accounting asymptotically correct shear deformation, *Journal of Applied Mechanics* 64 (1997) 905–915.
[38] W. Yu, D.H. Hodges, V.V. Volovoi, Asymptotic construction of Reissner-like composite plate theory with accurate strain recovery, *International Journal of Solids and Structures* 39 (2002) 5185–5203.
[39] W. Yu, D.H. Hodges, V.V. Volovoi, Asymptotically accurate 3-D recovery from Reissner-like composite plate finite elements, *Computers and Structures* 81 (2003) 399–454.
[40] W. Yu, Mathematical construction of a Reissner–Mindlin plate theory for composite laminates, *International Journal of Solids and Structures* 42 (2005) 6680–6699.
[41] J.-S. Kim, M. Cho, Enhanced first-order shear deformation theory for laminated and sandwich plates, *Journal of Applied Mechanics* 72 (2005) 809–817.
[42] J.-S. Kim, Reconstruction of first-order shear deformation theory for laminated and sandwich shells, *AIAA Journal* 42 (2004) 1685–1697.
[43] J.-S. Kim, M. Cho, Enhanced modeling of laminated and sandwich plates via strain energy transformation, *Composites Science and Technology* 66 (2006) 1575–1587.
[44] E. Reissner, On a mixed variational theorem and on shear deformable plate theory, *International Journal of Numerical Methods in Engineering* 23 (1986) 193–198.
[45] H. Murakami, Laminated composite plate theory with improved in-plane response, *Journal of Applied Mechanics* 53 (1986) 661–666.

[46] E. Carrera, C^0 Reissner–Mindlin multilayered plate elements including zig-zag and interlaminar stresses continuity, *International Journal of Numerical Methods in Engineering* 39 (1996) 1797–1820.
[47] E. Carrera, Developments, ideas and evaluations based upon the Reissner's mixed theorem in the modeling of multilayered plates and shells, *Applied Mechanics Reviews* 54 (2001) 301–329.
[48] E. Carrera, A study of transverse normal stress effect on vibration of multilayered plates and shells, *Journal of Sound and Vibration* 225 (1999) 803–829.
[49] A. Messina, Two generalized higher order theories in free vibration studies of multilayered plates, *Journal of Sound and Vibration* 242 (2001) 125–150.
[50] A. Messina, K.P. Soldatos, A general vibration model of angle-ply laminated plates that accounts for the continuity of interlaminar stresses, *International Journal of Solids and Structures* 39 (2002) 617–635.
[51] J.-Q. Tarn, An asymptotic variational formulation for dynamic analysis of multilayered anisotropic plates, *Computer Methods in Applied Mechanics and Engineering* 130 (1996) 337–353.
[52] W.Q. Chen, K.Y. Lee, Three-dimensional exact analysis of angle-ply laminates in cylindrical bending with interfacial damage via state-space method, *Composite Structures* 64 (2004) 275–283.
[53] K.M. Rao, H.-R. Meyer-Piening, Analysis of sandwich plates using a hybrid-stress finite element, *AIAA Journal* 29 (1991) 1498–1506.
[54] A. Benjeddou, J.-F. Deü, A two-dimensional closed-form solution for the free-vibrations analysis of piezoelectric sandwich plates, *International Journal of Solids and Structures* 39 (2002) 1463–1486.